Using COMSOL Multiphysics for Biomechanical Analysis of Stent Technology in Cerebral Aneurysms

J. Rasmussen[*,1], J. Thyregod[2], M.S. Enevoldsen[3], and K. Henneberg[3]
[1] COOK Medical Europe, Medicine & Technology- Department of Electro, DTU,
[2] COOK Medical Europe, [3] Medicine & Technology- Department of Electro, DTU
*Corresponding author: Joachimras@hotmail.com

Abstract: This work presents new fluid-structure interaction (FSI) models in both 2D and 3D of the effect of using vascular stents as treatment of cerebral berry aneurysms. The stent is positioned inside the cerebral artery covering the neck of the aneurysm. The stent is expected to alter the blood flow into the aneurysm such that the blood coagulates due to low blood velocity, and rupture of the aneurysm is prevented. A 3D FSI model consisting of three domains (blood, arterial, and aneurismal) is used to investigate the effect of the aneurysm on blood flow. Aspects of stent design such as pore size and shape and strut size, shape, and position are modeled in 2D and 3D FSI models. The models show that pore size and strut shape both have significant influence on stent efficiency.

Keywords: Cerebral aneurysms, vascular stent, fluid-structure interactions, strut setup.

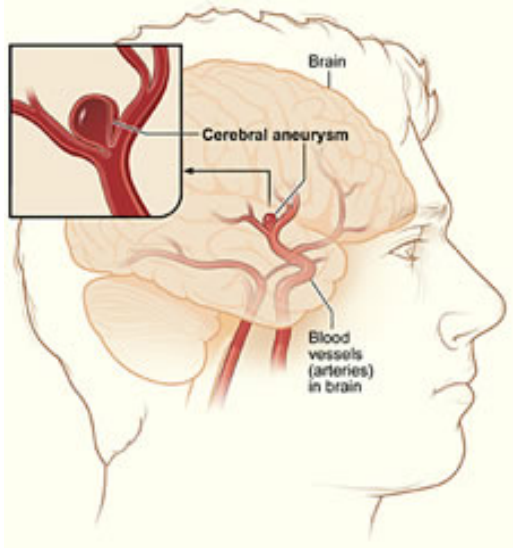

Figure 1: A cerebral berry aneurysm in the vasculature of the brain. Reprinted with permission from MUSChealth [17].

Author's note

This work has been performed in cooperation with COOK Medical Europe. Due to a non-disclosure agreement some of the results of this work have been anonymised.

1. Introduction

A cerebral aneurysm is an abnormal bulging of the arterial wall in the brain vasculature, see **Figure 1**. Two to five percent of the population in the industrialised world is expected to develop a cerebral aneurysm at some point during their lifetime [1]. Most aneurysms are not detected before they burst where they can cause bleeding into the structures of the brain or into the subarachnoid space (subarachnoid haemorrhage (SAH)). Each year approximately 30000 people in the U.S. are struck by SAH with mortality in the vicinity of 50%.

An aneurysm is defined as a focal dilation of the arterial wall. Especially the brain arteries are susceptible to aneurysms because the wall has different mechanical properties compared to other arterial wall. Among the risk factors for developing an aneurysm are smoking, hypertension and heavy alcohol consumption.
They can appear in patients at any age, but are typically found in persons at the age of 35-60 years. The risk of developing a cerebral aneurysm is higher for women than men by a ratio of approximately 3:2 [2].

When an asymmetric bulging of the arterial wall is present the aneurysm is said to be saccular. These types of aneurysms often arise in the cerebral vasculature at vessel bifurcations and appear on angiograms as a berry-like structure, hence the name berry aneurysm. More than 90% of all cerebral aneurysms are berry aneurysms, thus, this project will only focus on this type of cerebral aneurysms.

The berry aneurysm can range in sizes up to 30 **mm** in diameter [1,3] and has an almost spherical shape with a neck connecting the aneurysmal sack to the hosting artery. Usually berry aneurysms are treated by coil embolisation where thin platinum coils are introduced into the aneurismal cavity by catherterisation. The coils reduce the aneurismal blood velocity, invoking coagulation of the aneurismal blood volume, reducing the hemodynamic stress, and reducing the risk of rupture. In some cases a vascular stent is used in combination with the coils to ensure that the coils do not escape the cavity of the aneurysm. It has been reported that coagulation of the aneurismal blood volume is sometimes triggered by the stent alone without the introduction of coils. This suggests that a new specifically designed vascular stent may be used in aneurismal treatment. The hypothesis is that the vascular stent will redirect blood flow from entering the aneurysm, reducing the aneurismal blood flow sufficiently to trigger coagulation. This will reduce the hemodynamic stress on the aneurismal wall, and thus reduce the risk of rupture.

The vascular stent is composed pores surrounded by organised strut wires. The number and size of pores in the stent and the size, shape, and angle of the struts may all influence on the reduction of intra-aneurismal blood flow.

The purpose of this study is to use COMSOL Multiphysics to model the effect of different stent and strut designs in stent technology for treatment of cerebral aneurysms.

2. Model Setup

The anterior cerebral arteries (ACA) constitute the front part of the circle of Willis and are a common site for cerebral berry aneurysm formation. Especially the point where the anterior communicating artery (ACoA) branches off to join the two opposing anterior cerebral arteries is known to harbour berry aneurysms [3]. COMSOL Multiphysics 3.5 is used for simulation of blood flow in the ACA and berry aneurysms, as well as the effect of application of stents. The application of stents is only computed in 2D to keep the computation time low. The setup chosen for modeling is the ACA/ACoA branching with a berry aneurysm placed at the branching site. Shape, position, and setup of the struts in the vascular stent are incorporated into the models and the changes in blood flow are investigated.

Subdomain	Parameter	Value
Artery	Module	Structural Mechanics Module – Solid Stress-Strain
	Large Deformations	On
	Material Model	Hyperelastic Neo-Hookean
	Initial Shear Modulus	G=6204106**N**/**m**^{2} [5]
	Initial Bulk Modulus	κ=20·G [5]
	Density	ρ=960**Kg**/**m**^{3} [5]
Aneurysm	Module	Structural Mechanics Module – Solid Stress-Strain
	Large Deformations	On
	Material Model	Hyperelastic Mooney-Rivlin
	Density	ρ=960**Kg**/**m**^{3} [5]
	Material Parameter	c_1=15**N**/**cm**^{2} [6]
	Material Parameter	c_2=4**N**/**cm**^{2} [6]
Blood	Module	Chemical Engineering Module – Laminar Flow
	Material Model	Incompressible Navier-Stokes
	Density	ρ=1060**Kg**/**m**^{3} [5]
	Dynamic Viscosity	μ=0.005**Ns**/**m**^{2} [5]

Table 1. Subdomain settings for the model.

Boundary (Subdomain)	Parameter	Value
Inlet (Blood)	Velocity Mean Inlet Velocity Inlet Vessel Radius	$v_{mean}\cdot(1-y^2/R^2)$ v_{mean}= 36**cm**/**s** [12] R=0.9**mm** [18]
Outlet (Blood)	Pressure	P_{out}=7333**Pa** [19]
Internal Surface (Artery+Aneurysm)	Load	F_x=-T_x_chns F_y=-T_y_chns F_z=-T_z_chns

Table 2. Boundary conditions for the model.

2.1 Solid Domain Assumptions

Since the material constituents in the aneurismal wall differ from those of the arterial wall as described by *MacDonald et. al.* [4] it is necessary to apply different material properties to the two subdomains. Thus, the solid tissue domain of the model is divided into two subdomains - the arterial domain and the aneurismal domain. The arterial subdomain is modelled as a Neo-Hookean hyperelastic material whereas the aneurysm subdomain is modelled as a Mooney-Rivlin hyperelastic material.

The Neo-Hoookean hyperelastic material is described according to the strain-energy function [5]

$$W_s = ½\ G\ (I_1 - 3).$$

The only material parameter included in the Neo-Hookean strain-energy function is the shear modulus G and the only variable that is used is I_1 which is the first principal invariant of the right Cauchy-Green strain tensor.

The Mooney-Rivlin hyperelastic material is described by the strain-energy function [6]

$$W_s= c_1(I_1\text{-}3)+c_2(I_2\text{-}3).$$

This strain-energy function uses two material parameters c_1 and c_2 and includes two principal invariants I_1 and I_2 as variables. The increased number of material parameters and variables allows for a more precise and accurate material response that will resemble that of aneurismal tissue given the correct material parameters. The downside to this improvement in material response is an increase in computational time used by the FEM solver. The combination of the two differentiated material subdomains should therefore result in a detailed material response of the aneurismal subdomain while the simplification of the material model in the arterial subdomain should keep computation time by the FEM solver at a minimum.

2.2 Fluid Domains Assumptions

Blood is modelled in a third subdomain initially as an incompressible Newtonian fluid being fully developed when entering the ACA, resulting in a parabolic inflow profile and having an outflow pressure according to mean cerebral blood pressure [3]. Since the diameter of the ACA exceeds 0.5**mm** it is valid to assume blood as a Newtonian fluid as according to [7]. The size of the struts and gaps between the struts of a vascular stent lies in the vicinity of 60-200**µm**. Thus, when modeling how the vascular stent affects blood flow it is necessary to incorporate non-Newtonian behavior of blood into the models. The non-Newtonian behavior of blood is modeled according to the Carreau model, as [8]

$$\mu= \mu_\infty+(\mu_0- \mu_\infty)\cdot(1+K\gamma^2)^n,$$

where γ is the applied shear rate, μ_∞ is the infinite shear rate viscosity, μ_0 is the zero shear rate viscosity and K and n are parameters that determine the transition region. The Carreau model predicts a decreasing viscosity of blood for high shear rates. At high blood velocities where the shear rate is high the Carreau model exhibits a Newtonian behavior whereas for low shear rates at low blood velocities the model applies non-Newtonian behavior according to a power law fluid [9].

2.3 Anatomical Assumptions

Aneurysms appear in myriads of different sizes and shapes and because of this there exist

no measurements for a standard lesion. Therefore, a representative spherical aneurysm measuring 4**mm** in diameter is chosen.

The width of the neck is chosen arbitrarily, but kept above the neck-to-dome ratio of 0.5 which is the upper limit for aneurismal treatment with coil embolisation. By choosing an aneurysm with a neck wider than the neck-to-dome ratio of 0.5 it may be possible to asses which factors should be altered to affect the growth of aneurysms that are untreatable by coil embolisation.

In this paper only the bifurcation site of the ACoA (see **Figure 2**) is modeled. The ACA has an average diameter of 2.4**mm** and a wall thickness of approximately 0.3**mm**. The ACoA has an average diameter of 1.5**mm** and a wall thickness of 0.19**mm** [10]. Both sections of the ACA are specified to be 10**mm** in length whereas the ACoA is only 3**mm**. The angle between the distal part of the ACA and the ACoA is set to 90˚. Therefore the angle between the proximal ACA and ACoA as well as the distal ACA is 135˚, see **Figure 2**. The aneurysm is positioned in the wall of the distal ACA segment. The aneurysm has a diameter of 4**mm**, wall thickness of 50**μm** [11] and a neck-to-dome ratio of 0.8.

3. Use of COMSOL Multiphysics

The 3D model of the branching arteries and the berry aneurysm is constructed by the drawing tools in COMSOL Multiphysics. The two solid domains of the arterial and aneurismal tissues are defined using the Structural Mechanics Module whereas the blood domain is defined using the Chemical Engineering Module since this allows for laminar flow. The subdomain settings and the boundary conditions for the model is shown in **Table 1** and **Table 2** respectively.

For the simulations including a vascular stent the model is reduced to only 2D FSI models. The model geometries are similar to the 3D model and most boundary conditions are identical. The properties of the blood are defined using the Carreau model in the Chemical Engineering Module. The values for the Carreau model parameters are shown in **Table 3**.

Subdomain	Parameter	Value
Blood	μ_∞	0.00345**Ns/m^2**
	μ_0	0.056**Ns/m^2**
	K	10.976
	n	-0.3216

Table 3: Values for the Carreau model parameters. Values are obtained from [12].

4. Results

Figure 2 shows the blood velocity field in the 3D model. It is clearly seen how a jet of blood is caught inside the cavity of the aneurysm because of the position of the aneurysm. It is seen how the bifurcation of the vessels creates velocity profiles skewed towards the inside walls of the vessels in the ACoA and the distal section of the ACA, consistent with studies of blood flow in the carotid artery [13]. This effect and the position of the aneurysm create a large region with very low blood flow at the outside wall of the distal section of the ACA just after the bifurcation. If blood velocity in this region is sufficiently low, small blood clots can form at this site and travel with the blood stream with the risk of causing a stroke.

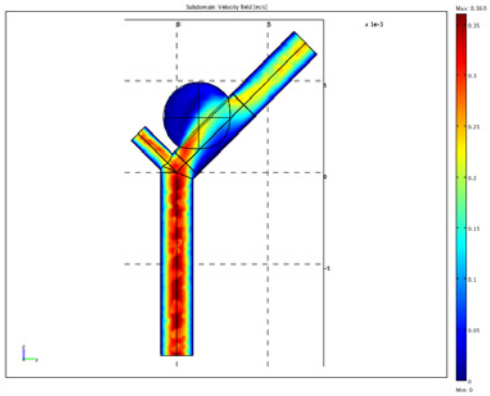

Figure 2: Simulated blood velocity field in the 3D model. Red colour indicates high blood velocity. Blue low velocity. Velocity range is 0.0-0.36**m/s**.

Close investigations of the blood velocity fields in **Figure 2** reveal local vortex areas inside the aneurismal cavity. The direction and velocity of the blood affects the vessel wall with a viscous force. By measuring the magnitude and direction of the viscous force vector in the aneurismal wall a measure for the magnitude and direction of the blood velocity vector is obtained. A reduction in the magnitude of the viscous force vector in the aneurismal wall would be a result of a reduction in the intra-aneurismal blood velocity.

Figure 3 shows the blood velocity field in the 2D stented ACA/ACoA model. The stent depicted in this figure incorporates square profiled struts of 100**μm** in diameter and 100**μm** diameter gaps. As seen from the figure, the presence of the stent substantially reduces the circulation of blood inside the aneurismal cavity. Blood velocity is furthermore reduced resulting in a decrease in wall shear stress and a reduced risk of rupture. By varying the shape, size and position of the struts and gaps in the stents optimal setups for blood velocity reduction can be found for this particular aneurysm.

Figure 4 shows the effect of strut shape and position in terms of the magnitude of the viscous force component on the aneurismal wall in a model including only the ACA segment with an aneurysm. All struts and gaps in the stents have the same diameter and position and it is clearly seen that the shape of the struts alone have a great effect on reducing the viscous force.

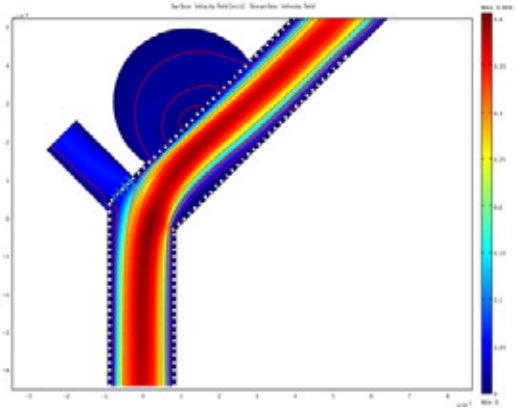

Figure 3: Blood velocity field in the 2D stented ACA/ACoA model including velocity streamlines. The jet of blood is kept from entering the aneurysm by the stent. Blood velocity range is 0.0-0.4**m/s**.

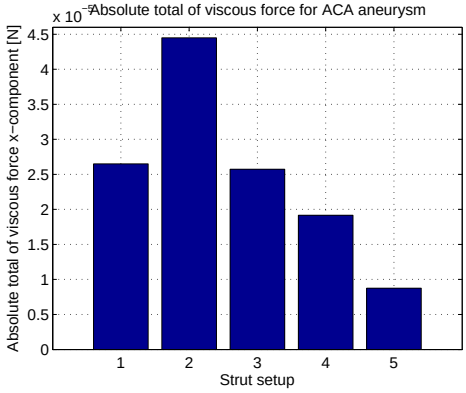

Figure 4: Viscous force in the aneurismal wall of the ACA model using differently shaped struts for the stent. All struts have the same diameter showing the effect of shape alone on reduction of the viscous force and blood velocity inside the aneurysm.

5. Discussion

The strain-energy functions describing the biomechanical properties of the vessel wall are the Neo-Hookean model for arterial tissue and the Mooney-Rivlin model for aneurismal tissue. By using hyperelastic strain-energy functions instead of linear elastic strain-energy functions the response of the model resembles more that of the human cerebral vasculature [14].

The Mooney-Rivlin function incorporates two material parameters whereas the Neo-Hookean function only includes one material parameter. This means that although more precise than the response from the linear elastic model, the material response of the arterial tissue is less accurate than the material response of the aneurismal wall. By incorporating more material parameters into the models by using e.g. a Fung type exponential strain energy function the material responses would have been even more precise for both the arterial and aneurismal tissues [1,14,15]. The simplification in the arterial and aneurismal tissue strain-energy function is chosen due to very long computation time.

Both the linear elastic models and the hyperelastic models assume that the wall materials are homogeneous and isotropic. The laminae of the arterial wall and the differentiated

tissues in the aneurismal wall clearly contradict this assumption. Studies of the arterial and aneurismal wall also show that the strength bearing collagen fibers found in the walls do not display an isotropic configuration [4,16]. Instead collagen fiber orientation changes within specific layers of the arterial and aneurismal walls giving rise to different material responses according to the direction of the applied loads. For more precise material models, anisotropic and heterogeneous material properties should be incorporated.

Even though the simplification of using 2D instead of 3D made it possible for the application of non-Newtonian behavior in the fluid domain, the downscale to 2D does reduce the accuracy of the model. By excluding the third dimension it is only possible to model a 2D configuration of the struts. When integrated into the mesh the complete stent is a 3D structure, so a thorough investigation of the strut design should be done in 3D.

Great efforts were made to apply non-linear behavior of the materials in the arterial and aneurismal walls, however, the non-linearity was not applied to the model where pore and strut design was tested, because this would lead to unreasonably long computation time. The interaction of blood flow on the solid non-linear structures of the arterial and aneurismal walls was used to draw an accurate picture of the complex velocity fields that are created by the aneurysm in the model. This insight was then used to base the stent design on reducing the blood flow into the aneurysm in the fluid models.

If the stent model had included the non-linear solid domains of the arterial and aneurismal walls, it would have been possible to investigate how the specific stent designs reduce the wall stresses in especially the aneurismal wall. This is relevant if the purpose of the stent design is aimed at immediate reduction of the aneurismal wall stress to prevent rupture. In this analysis of stent design focus was made on reducing intra-aneurismal blood flow to prevent aneurismal rupture.

The evaluation of the stent efficiency in this study was based on the viscous force components produced by the motion of blood close to the wall of the aneurysm. While giving detailed information on the hemodynamic changes on blood in the vicinity of the aneurismal wall, a good measure for intra-aneurismal blood flow is needed. The results of stent designs produced by the model do show reductions in the viscous force components and consequently the velocity of blood near the vessel wall. It must be assumed that alterations in the blood velocity near the aneurismal wall are linked to alterations in blood flow in the centre of the aneurismal cavity. The viscous force components can be used to display the presence of hemodynamic changes, but for a more precise measure alternative methods are needed.

6. Conclusion

The new FSI models in 2D and 3D show that a reduction in stent pore size allows less blood to enter the aneurismal cavity and thereby reduces the intra-aneurismal blood velocity. The FSI models further show that there is a great potential in improving stent efficiency by incorporating specific strut designs that alter blood flow. It is possible to drastically reduce aneurismal blood flow by reducing the pore size and using specific strut designs, reducing the risk of rupture to a minimum.

The next step in the modeling process will be to incorporate 3D FSI models incorporating 3D structures of stents e.g. by importing CAD drawings of stents. Patient-specific models should be constructed by extracting geometries from DICOM images. The models should be coupled with more precise material equations e.g. Fung-type materials and a pulsatile movement of blood to mimic the conditions of human tissue and blood.

While the geometry, response, and conditions are improved, a new method to measure the intra-aneurismal blood flow more precisely is needed. This could be used to precisely asses if the reduction in aneurismal blood flow caused by a specific stent design is sufficient to trigger coagulation of the aneurysm.

7. References

1. J.D. Humphrey & C.A. Taylor, *Intracranial and abdominal aortic aneurysms: Similarities, differences, and need for a new class of computational models*, Annu. Rev. Biomed. Eng., 2008(10), 221-246, 2008.
2. The American Society of Interventional and Therapeutic Neuroradiology (ASITN), Brain aneurysms and aneurysms information, May 2009, http://www.brainaneurysm.com/index.html.
3. M.J. Thubrikar, *Vascular Mechanics and Pathology*, Springer 2007.
4. D.J. MacDonald, H.M. Finlay, and P.B. Canham, *Directional wall strength in saccular brain aneurysms from polarized light microscopy*, Annals of Biomedical Engineering, 2005(5), 533-542, 2000.
5. COMSOL Multiphysics, *Structural Mechanics Module – User's Guide*, COMSOL, COMSOL 3.5 edition, 2008.
6. B.K. Toth, G. Raffai, and I. Bojtar, *Analysis of the mechanical parameters of human brain aneurysms*, Acta of Bioengineering and Biomechanics, 7(1), 2005.
7. C.M. Scotti, J. Jimenez, S.C. Muluk, and E.A. Finol, *Wall stress and flow dynamics in abdominal aortic aneurysms: finite element analysis vs. fluidstructure interaction*, Computer Methods in Biomechanics and Biomedical Engineering, 2008(3), 301-322, 2007.
8. F. Irgens, *Continuum Mechanics*, Springer, 2008.
9. COMSOL Multiphysics, Chemical Engineering Module – User's Guide, COMSOL, COMSOL 3.5 edition, 2008.
10. J. Sobotta, *Sobotta Anatomie des Menschen, Der Komplette Atlas in einem Band*, Urban & Fischer, 22nd edition, 2007.
11. J.D. Humphrey and S.L. Delange, *An introduction to Biomechanics – Solids and Fluids, Analysis and Design*, Springer, 2004.
12. A. Valencia, D. Ledermann, R. Rivera, E. Bravo, and M. Galvez, *Blood flow dynamics and fluid-structure interaction in patient-specific bifurcating cerebral aneurysms*, International Journal for Numerical Methods in Fluids, 2008(58), 1081-1100, 2008.
13. J.A. Jensen, *Estimation of Blood Velocities Using Ultrasound: A Signal Processign Approach*, Cambridge University Press, 1st edition, 1996.
14. J.D. Humphrey and S.K. Kyriacou, *The use of Laplace's equation in aneurysm mechanics*, Neurological Research, 1996(18), 204-208, 1996.
15. H.W. Haslach and J.D. Humphrey, *Dynamics of biological soft tissue and rubber: Internally pressurized spherical membranes surrounded by fluids.*
16. H.M. Finlay, P. Whittaker, and P.B. Canham, *Collagen organization in the branching region of human brain arteries*, Stroke – Journal of the American Heart Association, 1998(29) 1595-1601, 1998.
17. Medical University of South Carolina, Neurointerventional surgery – brain aneurysm, September 2009, http://www.muschealth.com/cerebrovascular/brainaneurysm.htm.
18. J. Alastruey, K.H. Parker, J. Pair, S.M. Byrd, and S.J. Sherwin, *Modelling the circle of willis to assess the effects of anatomical variations and occlusions on cerebral flows*, Journal of Biomechanics, 2007(40), 1794-1805, 2006.
19. M.J. Thubrikar, *Vascular Mechanics and Pathology*, Springer, 2007.